Ilkogretim Online - Elementary Education Online, Year; Vol 20 (Issue 4): pp. 285-299
http://ilkogretim-online.org
doi: 10.17051/ilkonline.2021.04.31

An experimental investigation of Al-Li alloy 8090 joint fabricated with friction stir welding (FSW) process by Taguchi-based DOE, for predicting thermal behaviour, mechanical and metallurgical characteristics

Raghuraj Panwar, Department of Mechanical Engineering, National Institute of Technology, Kurukshetra, Haryana (India)-136119, panwar.raghuraj@gmail.com
Dr.Pankaj Chandna, Department of Mechanical Engineering, National Institute of Technology, Kurukshetra, Haryana (India)-136119, pchandna08@gmail.com

Abstract- In this exploration study, friction stir welding of Al-Li 8090 alloys has been accomplished for the optimization of process parameters for determined joint strength. Taguchi's L_9orthogonal array (OA) has been used for different three parameters-tool rotational speed, tool traverse speed, and dwell time. To optimize, multi-response had been carried out through Taguchi's-based design of expert. It has been designed for all three responses–ultimate tensile strength, and micro hardness, microstructure. Thermal behaviour analysis shows the temperature variation during friction stir welding at different parameters. Analysis of variance has been used as a tool for obtaining DOE-OA to determine the significant process parameter. Tool traverse speed and dwell time has been predicted the two utmost significant parameters which influence extreme quality features of joint by friction stir welding. Validation of the probable value obtains by confirmation experiments at optimal sets shows the worthy agreement with the values of the experimental outcomes.

Keywords: Friction stir welding; DOE orthogonal array; analysis of variance;thermal behaviour analysis;SEM, micro-hardness; ultimate tensile strength.

I. INTRODUCTION

Reinforced metal matrix composites for nano particles are commonly used for aerospace and automobile applications. In all applications where weight reduction will be the key point in the excellent of manufacturing materials, Al-Li alloys include high strength and light weight alloys that can be used for welded construction [1]. In contrast with composite materials, which on the other hand, exhibit more convenient weight, but higher manufacturing costs, these alloys can also be economically efficient with decreased density and improved young modulus.The solidification temperature range becomes shorter when Li is over the solubility limit, and more eutectic constituents has been available in the last stage of solidification to healing all produced cracks, to some extent. In such a way, the risk of developing cracks should be less in both low and high Li content.

Fortunately, many Al-li alloys, such as the 8090 alloys considered here, are constructed with the main purpose of improving mechanical properties, so minor composition can result in a peak susceptibility to cracking. Since these alloys are more susceptible than other Al-alloys to welding solidification cracks due tothe hygroscopic nature of Li-containing aluminum oxides, weld porosity would be another specific issue for Al-Li alloys.Thus, by extracting a surface layer of around 0.1 mm, a reduction in tensile strength may be submitted to an appropriate cleaning method or, better, to a mechanical milling. This activity will substantially decrease the presence of porosity . For sample, when Li is about 2.5 percent in weight, crack susceptibility for a binary Al-li alloy has been evaluated to be maximum[1].

In the literature focused on the Al-Li alloys, many studies concentrate in order to minimize its weight, the aerospace industry encourages research for new materials. Reducing the use of petrol. Aluminium-Lithium alloys have become a good choice because of their intrinsic existence properties. Nonetheless, using conventional welding to join these materials is difficult. Due to the low heat input, the friction stir welding method is considered an ideal joining process for these materials [2]. Microstructural and mechanical properties of the 2060 Al-Cu-Li alloy joints of 2.0 mm thickness obtained at various joints.This research measured rotation speeds ranged from 400 to 1300 rpm with welding constant speed of 100 mm/min is maintained. Grain coarsening with the rise in the speed of rotation occurred when precipitation density decreased[3]. The purpose of the current work is to study the formation of fine

grains during the transformation of a process of a AA 8090, thermo-mechanically treated The alloy is exposed to thermomechanical treatment during friction stir welding (FSW). Friction stir welding (FSW) was performed by varying the parameters and the TTS 800, 1000 and 1200 rpm rotation speed, 2.5 mm/s welding speed and 5000 N axial force[4].Aluminum-lithium alloys have been used commonly in aircraft and aviation area of aerospace. It is now one of the essential materials for the manufacture aircraft in China at large scale. One of the main strategies for solving the complexity of the precise deformation of Al-Li alloy pieces is thermoplastic deformation. A phenomenological approach characterizes the thermoplastic deforming behavior of the Al-Li alloys. The impacts of temperature deformation, strain rate, and combination with in the model, strain is applied to match and predict the flow pressure[5].

Y. Tao, Z. Zhang [6] revealed that the lowest hardness zone (LHZ) has been located at the heat affected zone (HAZ) for friction stir welded (FSW) joints of standard precipitation-hardened aluminum alloys and determined the tensile fracture behavior with the fracture occurring at the LHZ. However, for FSW 2060-T8 joints, the LHZs were located below 400 rpm-200 mm/min at the nugget zone (NZ), but under 800 rpm-200 mm/min at the HAZ, 1200 mm/min at the HAZ.Huijie Liu [7] analysed of the 2060-T8 Al-Li alloy friction stir welded for the present work using the rotation speed range of 600-1000 rpm has been summarized at a steady welding speed of 300 mm/min. It has been investigated the effect of rotation speed on the microstructure and the mechanical properties of the joint.The optimum intensity was attained at the speed of rotation 800 rpm. The overall elongation, however, is just 2.8 by percent. A model is designed to describe the mechanism of the crack is initiated and propagated in a joint of the material systems considered. In relation to the BM with different precipitates have been found in the WNZ, with only small quantities of T1, β and δ. That contributes to the decrease the mechanical properties.

II. MATERIALS AND METHODS

2.1 Experimental arrangement

Aluminium 8090 with 5 mm thick plates was selected for experimentation in this sample. Table 1 indicates the findings obtained during the OES study (Fig. 1) carried out to determine the composition of the work piece. The test specimens (100 mm x 75 mm x 5 mm) were taken from a plate measuring 320 mm x 320 mm x 5 mm. In addition, before starting the FSW process, the plate surface was machined with the help of VMC to prevent dislocation of work plates during welding. High speed steel (H-13) instrument with cylindrical thread and concave shoulder was used, as shown in Fig.2 during experimentation.

Table 1. Chemical Composition of 8090 Al-Li alloys (in weight %)

Elements	Percentage
Li	3.07
Cu	1.37
Mg	0.733
Zr	0.103
Ag	0.28
Zn	<0.25
Mn	<0.59
Al	**Bal.**

Any other trace element has a max. wt. percent of 0.05 and not to exceed 0.15(max) for the max. of all trace elements

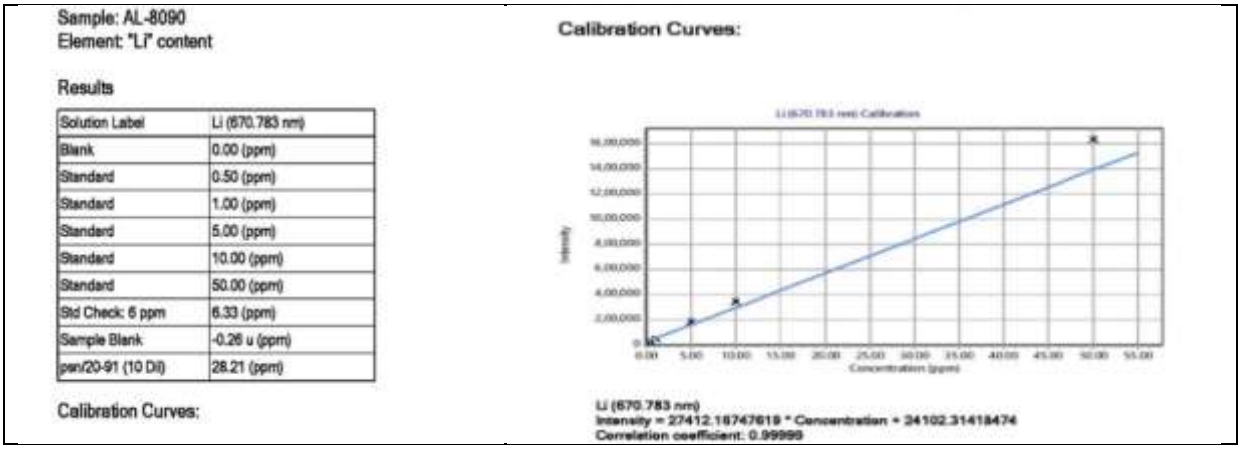
Sample: AL-8090
Element: "Li" content

Results

Solution Label	Li (670.783 nm)
Blank	0.00 (ppm)
Standard	0.50 (ppm)
Standard	1.00 (ppm)
Standard	5.00 (ppm)
Standard	10.00 (ppm)
Standard	50.00 (ppm)
Std Check: 6 ppm	6.33 (ppm)
Sample Blank	-0.26 u (ppm)
pan/20-91 (10 Dil)	28.21 (ppm)

Calibration Curves:

Figure 1. Li fraction present in AL-8090 alloy

Figure 2. Tool profile

2.2 Experimental procedure

The vertical milling machine having a bed dimension of 200mm x1300 mm and with a speed of 500 to 3000 rpm has been driven by four-step pulley arrangement which was used to perform a job with the help of fabricated fixture, as shown in Fig.3. High-speed steel (H-13) grade has beenused for tool during this FSW process. For Al-LI-8090, the geometry of the shoulder diameter and tool pin was used as a welding parameter.Accordingly with the help of lathe machine , tool was reduce to 16 mm from the maximum diameter of tool materialas requirement parameter of the toolneeded,which has been mandatory by the design of experiments (DOE). The tool with cylindrical threaded tip has been annealed and oil quenched for hardening the tool material after manufacturing. The joint consisted of a total of nine experiments with respect totool transverse speed, tool rotation speed, dwell time (Obtained from pilot experiments) on the material Al-Li 8090 under atmospheric conditions. All three parameters and the architecture of the experiment were generated by Taguchi's static design with L9's DOE orthogonal array (OA). The experiment sample taken out for the tensile test performed by nine experiments was shown in Fig. 4 (a, b and c).The experimental conditions used during the run of experimentation are shown in Table 2.The various L9 OA values of Taguchi that have been used for this experimental method has been display in Table 3.

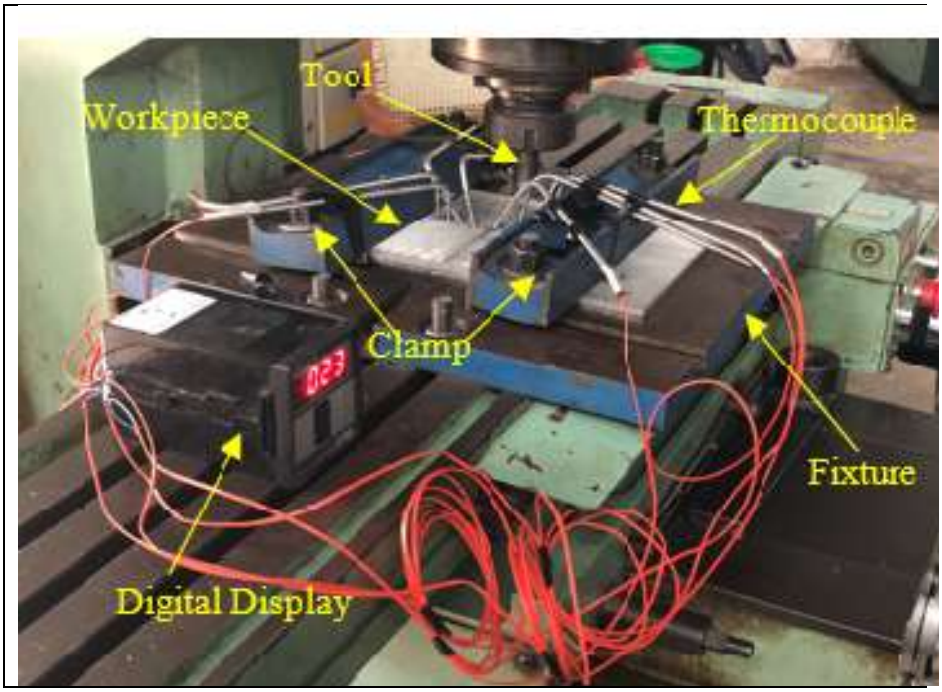

Figure 3. Experimental test rig

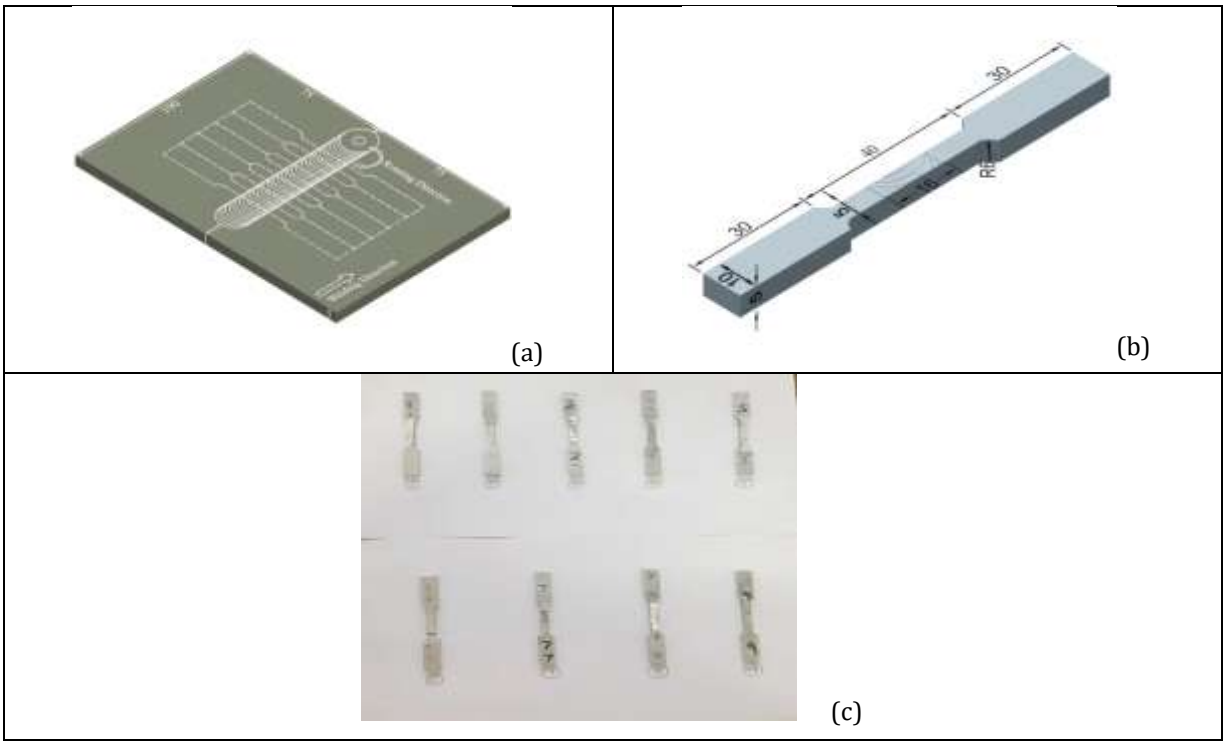

Figure 4. (a ,b) Labelled diagram for UTS test samples (c) photograph shows dog bone shape sample from welding plates.

Table 2. Experimental conditions

Experimentation	Designation	Conditions	Process Parameter
FSW	FSW-A	under Atmospheric	Tool Rotation Speed(rpm)
			Tool Transverse speed (mm/min.)
Taguchi			Dwell Time(sec.)

Approach(L9)

Table 3. Experimental and process considerations using Taguchi's L-9 standard OA for UTS

S.no	TRS (ω) (A)	TTS (WS) (υ) (B)	DT (s) (C)	UTS (MPa)	Micro hardness (avg.)	S/N ratio UTS	S/N ratio Micro hardness	Heat Input Index $\omega^2/\upsilon\times10^{-4}$(HI)	Order
1	710	16	7	235	106.46	47.4214	40.5437	3.1506	5
2	710	25	14	201	89.21	46.0639	39.0083	2.0164	8
3	710	40	21	227	105.41	47.1205	40.4576	1.2602	6
4	1000	16	14	243	94.68	47.7121	39.5252	6.2500	4
5	1000	25	21	245	104.58	47.7833	40.3890	4.0000	3
6	1000	40	7	200	87.37	46.0206	38.8272	2.5000	9
7	1400	16	21	248	89.90	47.8890	39.0752	12.250	2
8	1400	25	7	265	115.81	48.4649	41.2749	7.8400	1
9	1400	40	14	205	106.50	46.2351	40.5470	4.9000	7

The arrangement of tool traverse and speedof tool rotational used in the existingsurvey and their associated sample to optimize the welding for the selected tool presented in above mentioned table (no.3) with the heat index [8][9], which has been a depiction of the average value of thermal contour at the time of welding. The rotational speed, the welding tool transverse speed, dwell time and tilt angle were 1400rpm, 25 mm/min, 7sec. and 0^{o}, respectively displayhigher UTS and Micro-hardness values with a shoulder diameter 16mm with athreaded cylindrical tool pin. Sodium hydroxide mixture (20gNaOH+100ml H_2O) has been used to eliminate the undesirable material caught near the tool at the moment of experimentation.

2.2.1Taguchi design for experiments

The Taguchi design process uses fractional factorial test design called OAs that assist to reduce the trial number of experiments. The choice of the appropriate OA depends on thenumber of control factors and their levels. By using OA design technique, multiple processvariables can be estimated which simultaneously affect the systems characteristics whilereducing the number of test runs. For example, for four parameters at three levels, thetraditional full factorial design would have been required 34 or 81 experiments. In the TaguchiL 9 OA, however, the necessary experiments in Taguchi L 9 orthogonal array are only 9. Toachieve this goal, the design of Taguchi L 9 OA (four factors with 3-level design) was used todetermined and optimize the instrumental parameters which have been consider the precisionstrength of welds and joints. The design of the experiment (DOE) using for the Taguchimethod provides a simple, effective, and organized approach for the determination ofoptimum conditions. With the aim to lessen the number of experiments to be performed, the fractional factorialassessment strategy is adopted during 'Taguchi design' procedural which is defined as OAs.The suitable selection of OA is dependent on control factor including levels associated withit. It calculates multiple process variables which impart effect on the features of system.Likewise, the conventional design of full factorial with 4 parameters by 3 levels may havethirty-four or eighty-one try outs. During Taguchi L 9 OA approach, the number of trials isnine. Furthermore, an optimised condition is achieved for the designing of (DOE) proceduralwith application of Taguchi approach.

2.3 Thermocouple arrangement

Thermocouples (K-type) have been mounted to predict the total temperature at different positions at a distance of 10 mm on both RS and AS surfaces, as shown in Fig. 5 (a, b).Thermocouples have been

connected to a digital display unit for the display of temperature. It also consists of a system for the transfer of data through the use of thermocouples indata recorder termed a channel interface units.

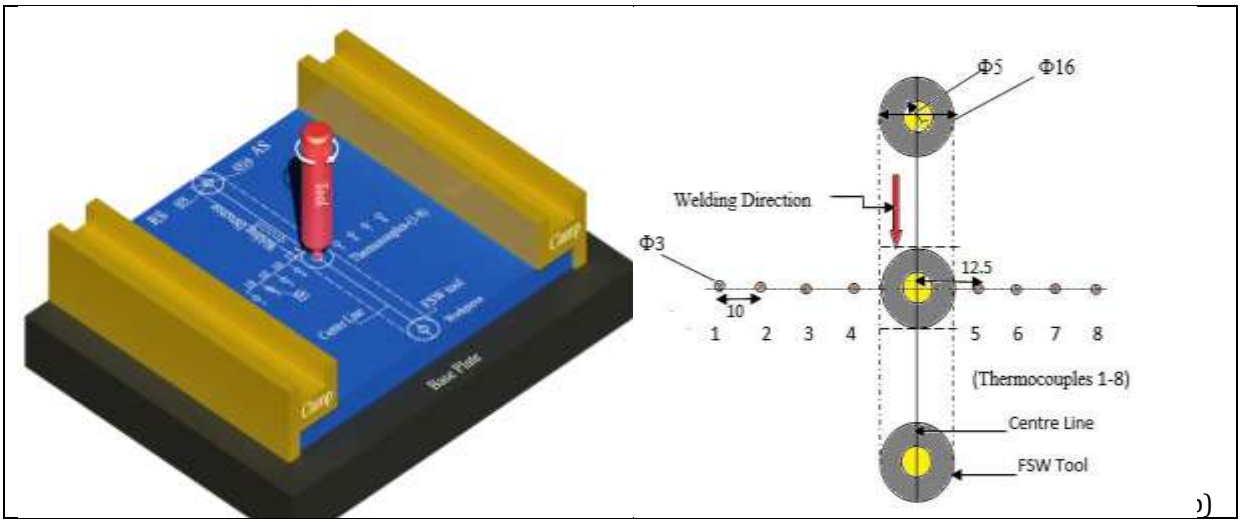

Figure 5. (a) Schematic diagram of the FSW fixture (b) Thermocouple location within the work-piece

For each experimental condition, thermocouples were attached to the centre of the plate, four thermocouples were engaged on the retreating side (RS), while another four were engaged on the advancing side (AS). In order to avoid thermocouples from becoming disassembled throughout the welding phase, the first thermocouple was positioned at a distance of 12.5 mm from the midline on both surfaces.Here, eight extraordinary L-shaped k-type thermocouples with a 3 mm diameter pointing nose tip were attached to the workpiece surface in plates by a drilled hole at a 10 mm distance on both the retreating side (RS) and the advancing side (RS) (AS). This enables the showing of proper temperature changes on the digital display unit. The diameter of the drilled hole is up to 4.7 mm as the total thickness of the plate is 5mm to escape the base contact among the tip of the thermocouple and the base plate.

2.4 Mechanical and micro-hardness testing

The sample of tensile has been cut from the welded plate vertical to the welding direction as illustrated in Fig. 4(a). Samples of tensile have been made as per standard of ASTM-E8. In particular, the rectangular strip (100mm ×75mm×5mm) has been cut out from the sample of welded joint by using a power hacksaw machine. After this process, these sample strips have been transformed into a sample for the tensile test by utilizing an end-mill cutter and the size of the sample has been shown in the Fig. 4(b), the testing of tensile has been carried out by UTM (made: Fuel Instruments and Engineering Pvt Ltd) for the calculation of strength of tensile and percentile elongationof joint by FSW (strain rate in mm/min.). Samples for micro-hardness test have been taken into strips of rectangular shape (22mm×6mm×5mm) from the centre line of welded plates as shown in Fig. 6. After that emery paper of grit size 400, 600, 800, 1200, 1500, and 2000 has been used to maintain uniformity in the upper and lowest surface of samples to prevent defects at the time of measurement. As a result high refractive and scratch-free surface by cloth polishing has been done. To conclude, these specimens were analysed with Vickers Micro-hardness at 100g load.

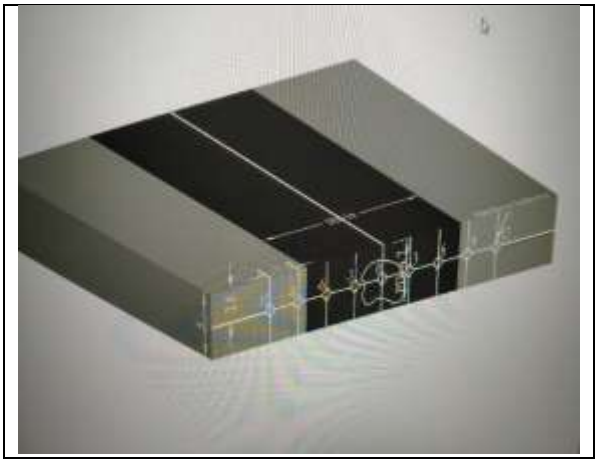

Figure 6. Schematic diagram for different intender location for Micro-hardness testing.

The welded dog bone shape samples that have been used for conducting experimentation has been shown in Fig 4(c). After the tensile testing breaking of test samples from the welded zone has been observed and the same has been depicted in Fig. 7.

Figure 7. Photograph of the broken welded sample by UTM.

2.5Micro-structural Observation

Sample made of the metallurgical study have beenfound similar to micro-hardness. After polishing by cloth, prepared samples wereitched by Keller's reagent which constitutes of themixture of 90 ml pure water, 1.5 ml of HCL, 2.5 ml of $HNO_3$and 1 ml of HF. Later the specimen has been checked at the microscopic andmacroscopic level with the aid of optical microscopic and scanning electron microscopy(SEM), respectively. The different welding zones were visualized by Optical Microscope. Lastly, the fracture surface of tensile specimens has been analysed by scanning electron microscopy (SEM) for Fractography analysis.

III. RESULT AND DISCUSSION

3.1Thermal analysis

During FSW, the thermal phase has been accomplished in four steps, plunge time (PLT), dwell time (DT), process time (PT), and pull-out time (POT). Atthe first step of plunge time (PLT) the cylindrical pin penetrates in between lines joiningthe two plates. Throughout dwell time, after penetrating the rotating tool between two plates, the tool has been kept continuously rotating at the initial point without any transverse moment. The time engaged to accomplish the welding was called as process time. Whereas the time engaged to exit the rotating pin from the weld zone after the execution of the process termed as pull-out time. These processes has been illustrate in Fig. 3.

In the present research, it has been marked that pin penetrates time stood the 20s, dwell time 30s, process time 80s, and pin pull out time remained 20s. During FSW, the heat influence was an outcome of the friction between the tool and workpiece, which enhancesthe temperature growth in the stir zone (SZ). The heat considerably affects the metallurgical and mechanical properties of the welded joint of annealed alloys [10, 11]. The thermal cycle thus plays an important role in complete welding excellence.

It has been observed for all the cases that has been consider for present experimental work that after a dwell period tool moves in the direction of welding ,the temperature rises steadily and observed maximum in middle and it again start decreasing as the tool leaves from centre of work piece. A non-symmetrical temperature profile has been observed for all the cases. Further temperature corresponding to retarding side has been named as T1,T2,T3, and T4 respectively and T5,T6,T7, and T8 are for Advancing side as shown in figure 5(b).The results highlighted that out of all the temperature values, the temperature corresponding T1and T8 has been recorded minimum values where as T4 and T5 are the maximum value of temperature recorded. The reason being, the temperature variation has been more on RS and less on Advancing side because of the moment of material from AS to RS side due to tool pin rotation.

The thermal analysis during FSW has been carried out under different experimental conditions of TRS, TTS, DT (case 1 to 9) and represented graphically as depicted below.

3.1.1 Case 710,16,7

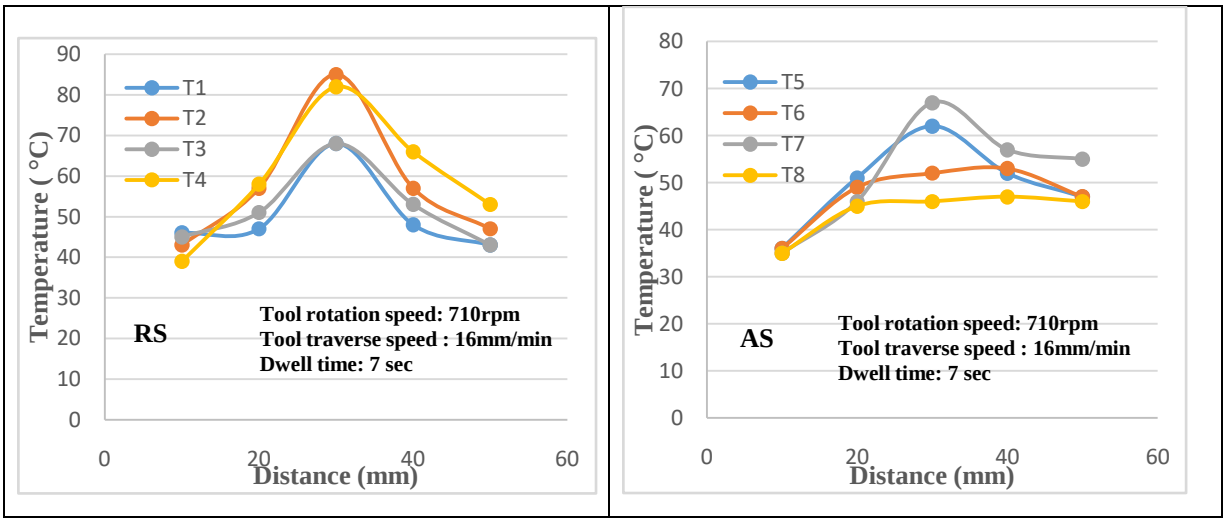

(a) (b)

Figure. 8(a) and 8(b), graph plot for temperature measuring on a different location for thermal analysis, case (710,16,7).

3.1.2 Case 710, 25, 14

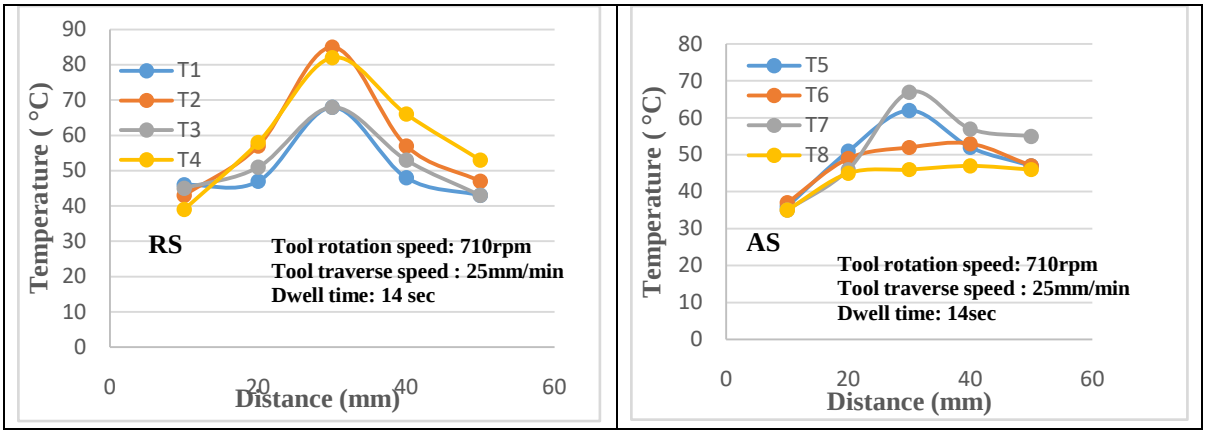

(a) (b)

Figure. 9(a) and 9(b), graph plot for temperature measuring on a different location for thermal analysis

3.1.3Case 710, 40, 21

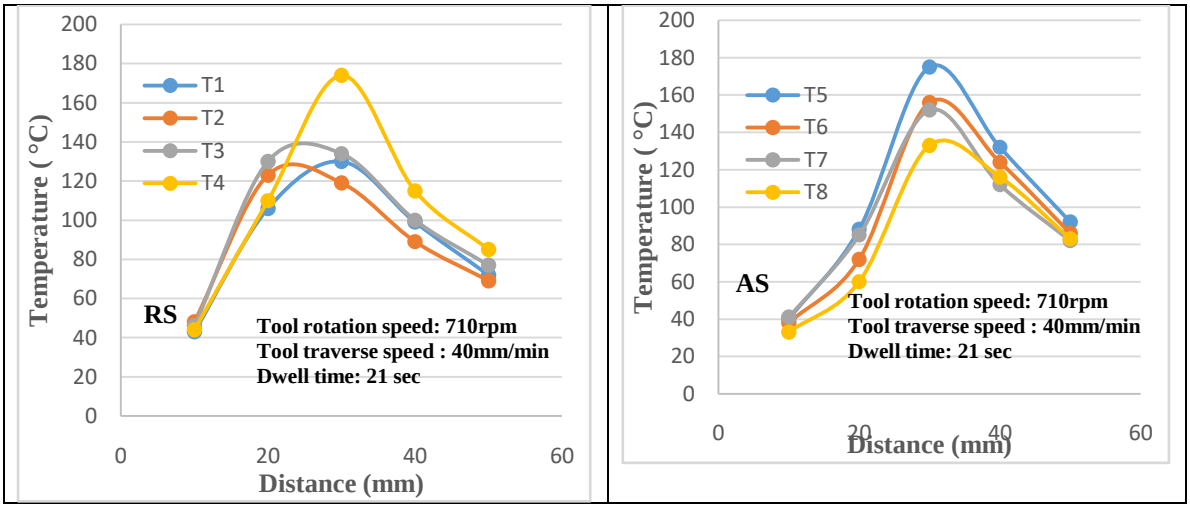

(a) (b)

Figure. 10(a) and 10(b), graph plot for temperature measuring on a different location for thermal analysis

3.1.4 Case 1000, 16, 14

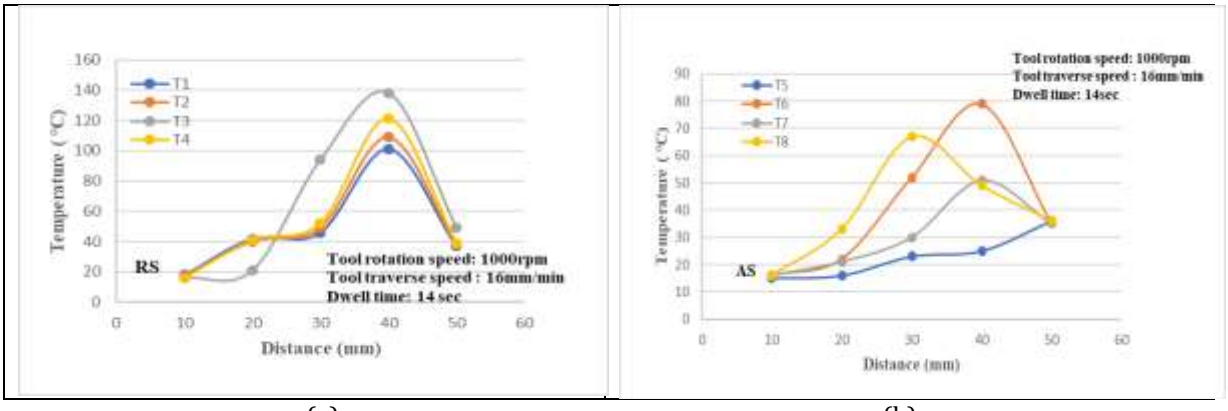

(a) (b)

Figure. 11(a) and 11(b), graph plot for temperature measuring on a different location for thermal analysis

3.1.5 Case 1000, 25, 21

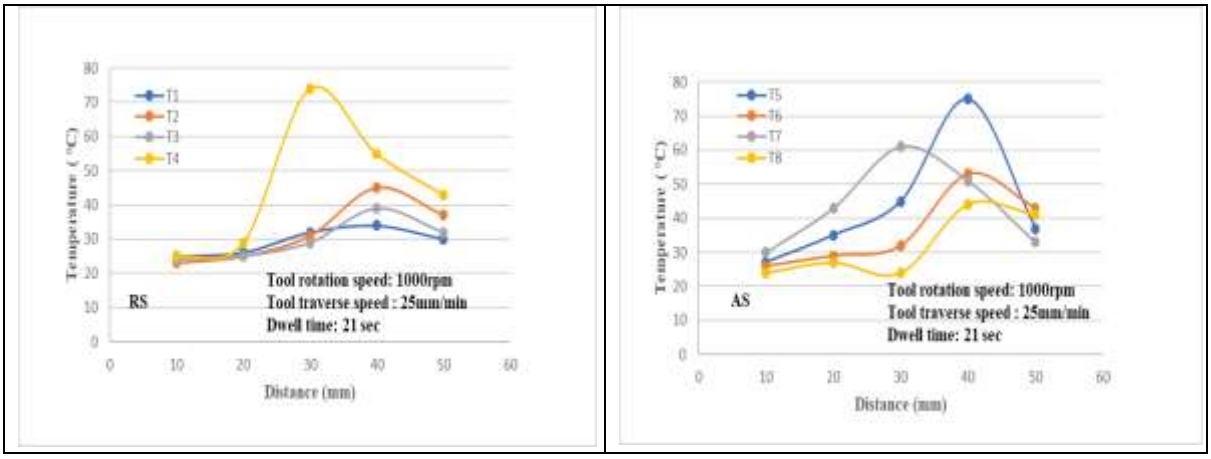

(a) (b)

Figure. 12(a) and 12(b), graph plot for temperature measuring on a different location for thermal analysis

3.1.6 Case 1000,40,7

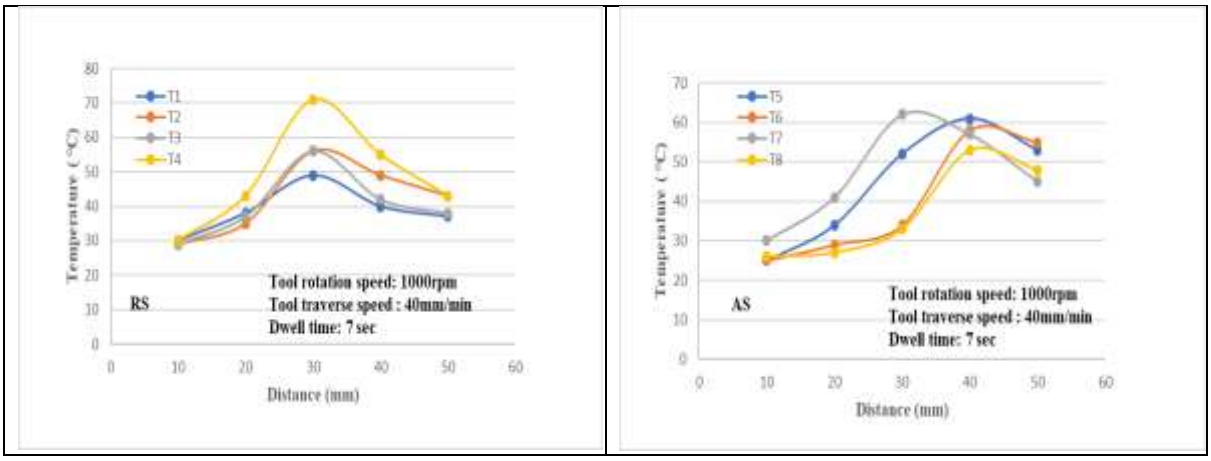

(a) (b)

Figure. 13(a) and 13(b), graph plot for temperature measuring on a different location for thermal analysis

3.1.7 Case 1400, 16, 21

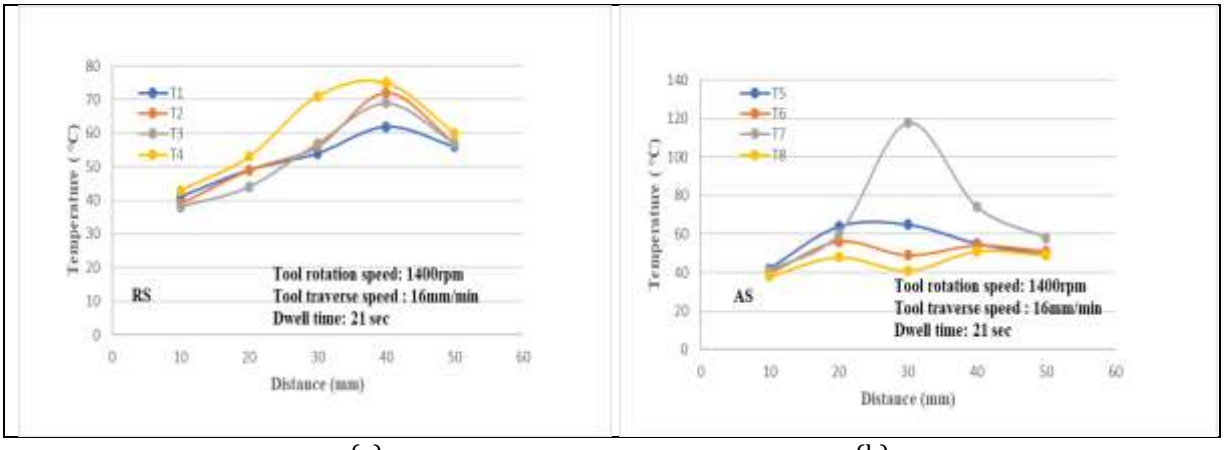

(a) (b)

Figure. 14(a) and 14(b), graph plot for temperature measuring on a different location for thermal analysis

3.1.8 Case 1400,25,7

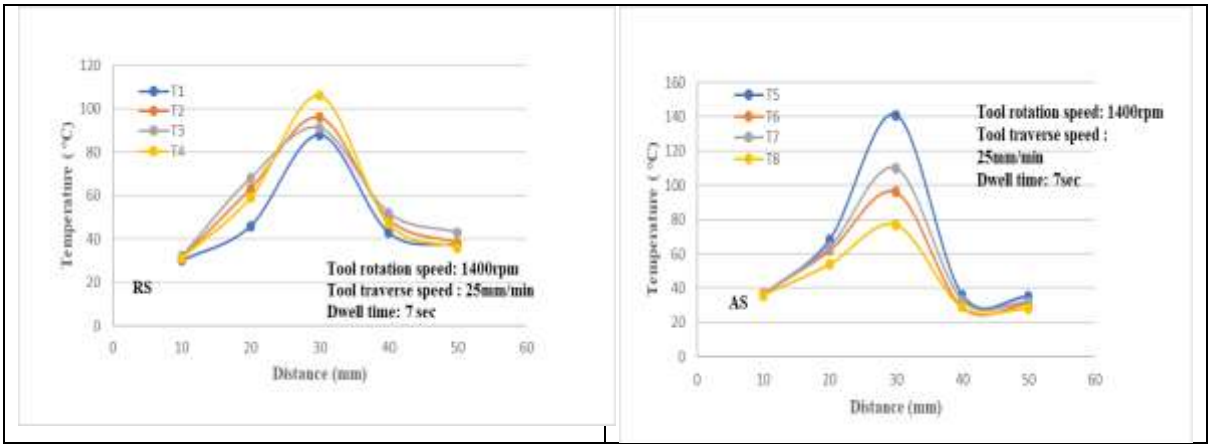

(a) (b)

Figure. 15(a) and 15(b), graph plot for temperature measuring on a different location for thermal analysis

3.1.9 Case 1400, 40, 14

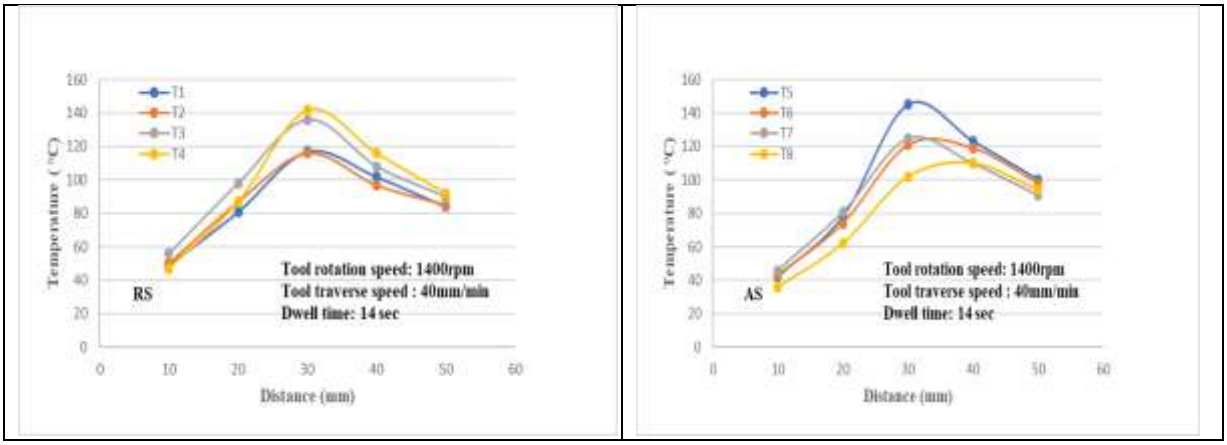

(a) (b)

Figure. 16 (a) and 16 (b), graph plot for temperature measuring on a different location for thermal analysis

3.2SEM analysis

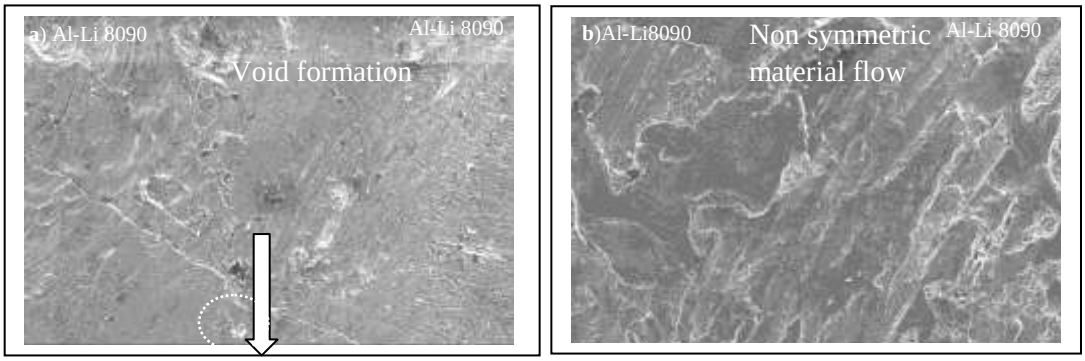

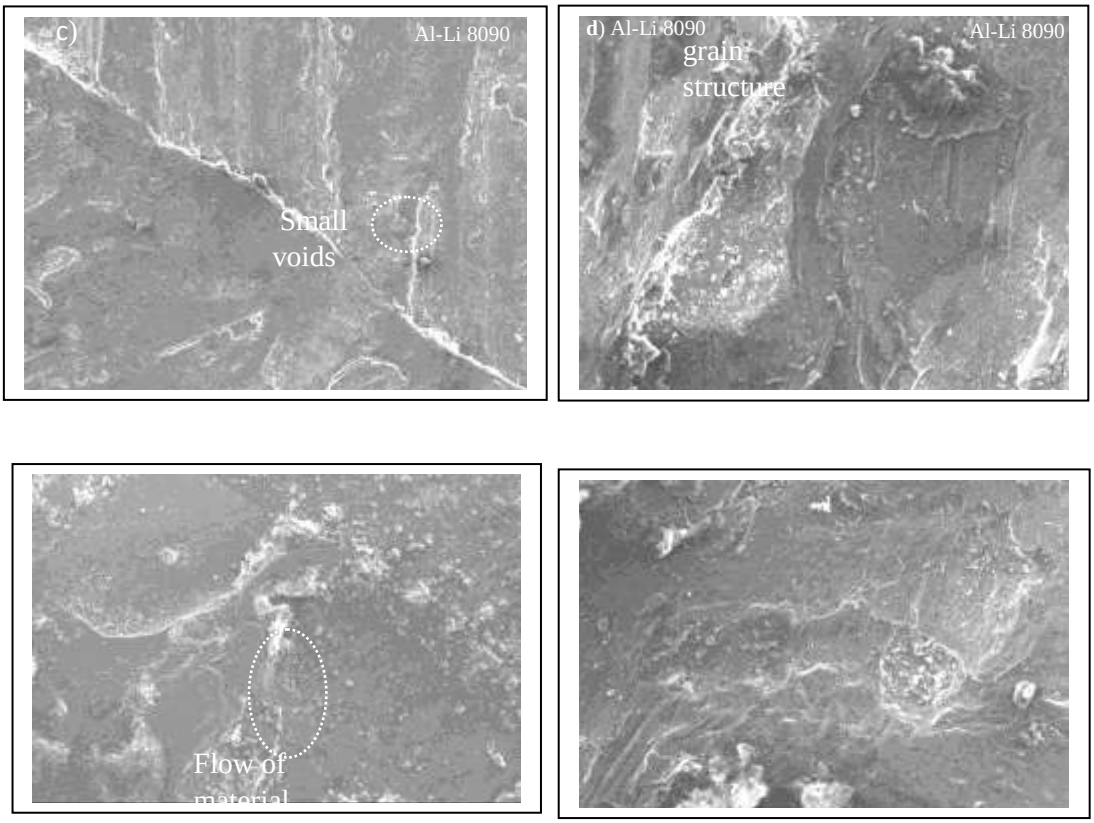

Figure.17 SEM images of the precipitated phase in Al-li 8090 and welding regions of the joint at TRS 1400 rpm, 1000 rpm, and 710 rpm on different TTS and DT.

3.3. Tensile Testing under different welding parameters

The results of the study revealed in Table 3. The parent metal observed the maximum tensile strength as 514 MPa. The tensile strength of the fabricated welding joint was attaining 265 MPa which predicted 51.5 %strength of the base metal. The resulted decrement in the strength was due to the low density and dissolution in NZ participation due to the dynamicrecrystallization[12]. The deprivation of mechanical properties was intended to increase by the use of a cylindrical threaded tool. The tensile characteristics of the joint with different welding conditions has been presented in Table 3. It has been shown in Table 3, that the welding joint of the platein case TRS-1400 rpm, TTS-25mm/min, and DT-7 sec. having maximum tensile strength obtain by cylindrical threaded tool over the normal tool at a tilt angle 0˚.

As we seen in Fig.18(a),Taguchi analysis predict that the main effect of mean of S/N ration has been constantly increase as TRS 710 rpm SN value shown 46.85, it increase at TRS 1000 rpm the SN value 47.20 and maximum at 1400 rpm that has been shown 47.60. Here we see that the value on different TTS, SN ration constantly increases. While during TTS 16 mm/mintheSN value shown 47.65 and decrease at TTS 25 mm/min the SN value shown to 47.45 and minimum at 40 mm/min the SN value 45.40, it has been evidence that at minimum TTS highest SN ration predict in Fig.18 (a) and SN ratio decrease while TTSincrease constantly**.** In DT at 7 second value of SN ratio is 47.35 it decrease at 14 second to SN ratio 46.60 and again increase at 21 second to SN ratio to 47.60.This plot (18a) clearly evident that while TRS-1400(SN 47.60),TTS-25(SN 47.45) and DT-7(SN 47.35), and shows the best optimum results for this research because all values lies above the middle line of SN ratio graph,which had been consider for case 8 in Table 3. Here in response Table 4, signal to noise ratio(larger is better)we consider for this experimentation, hence, TTS and DT has been consider the best ranki.e first and second, respectively. Fig.18 (b) shows main effect of mean of means.

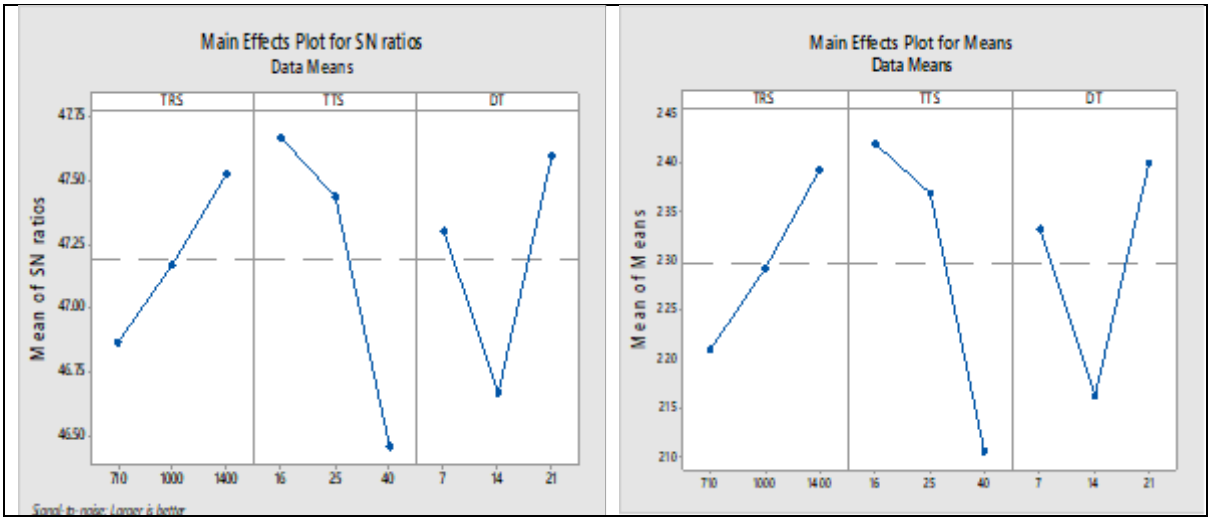

Figure 18(a, b). Plots of signal-to-noise-ratio andthe main effect of Mean of Means

Table 4. Response table for Signal to Noise Ratio (Larger is better) and Means.

Response Table for Signal to Noise Ratios (Larger is better)			
Level	TRS	TTS	DT
1	46.87	47.67	47.30
2	47.17	47.44	46.67
3	47.53	46.46	47.60
Delta	0.66	1.22	0.93
Rank	3	1	2

Response Table for Means			
Level	TRS	TTS	DT
1	221.0	242.0	233.3
2	229.3	237.0	216.3
3	239.3	210.7	240.0
Delta	18.3	31.3	23.7
Rank	3	1	2

3.4 Micro-hardness Testing

Micro hardness of Al-Li 8090 alloy is calculated at the rectangular area of (22mm×6mm×5mm) piece of friction stir welding on different positions. An average of six readings taken at a distance of 3 mm from the top surface of welding has been reported. The variation of micro-hardness has been plotted against the distance. Micro-hardness variation in the 8090 series was interrelated with grain, precipitate density. Plastic deformation and intense heat in NZ reduces the grain size of NZ as compared to TMAZ and HAZ. Therefore, NZ shows the higher microstructure than the close region, which was covered under the Half-Petch Equation [13].C. Muralitharan et al.[14]reported that a more hardness value of NZ was related toincreased dispersal precipitate density which further increases hardening process due to natural aging.

Here in Fig.19 (a) S/N Ratio shows that at TRS 710rpm S/N value predicts 41 and at 1000 rpm it decreases to 39.59 while it rises to 40.2 at 1400 rpm which has been shown maximum. But during TTS at 16 mm/min value shows 39.75 and slightly increases at 25mm/min to 40.23 and then decreases at 40mm/min to 39.92. However, S/N value at dwell time predicts highest at 7s to 40.2 and decreases at 14 s to 39.7 and again increases at 21s to 39.95. Whereas means of mean effect shows in Fig.19 (b) has been similar to the S/N ratio. Hence we can say that the S/N ration at TRS 1400rpm, TTS 25mm/min, and DT 7s has been the highest range of input parameters. The delta rank shows in Table.5 that TRS, DT and TTS predict first, second and third rank accordingly.

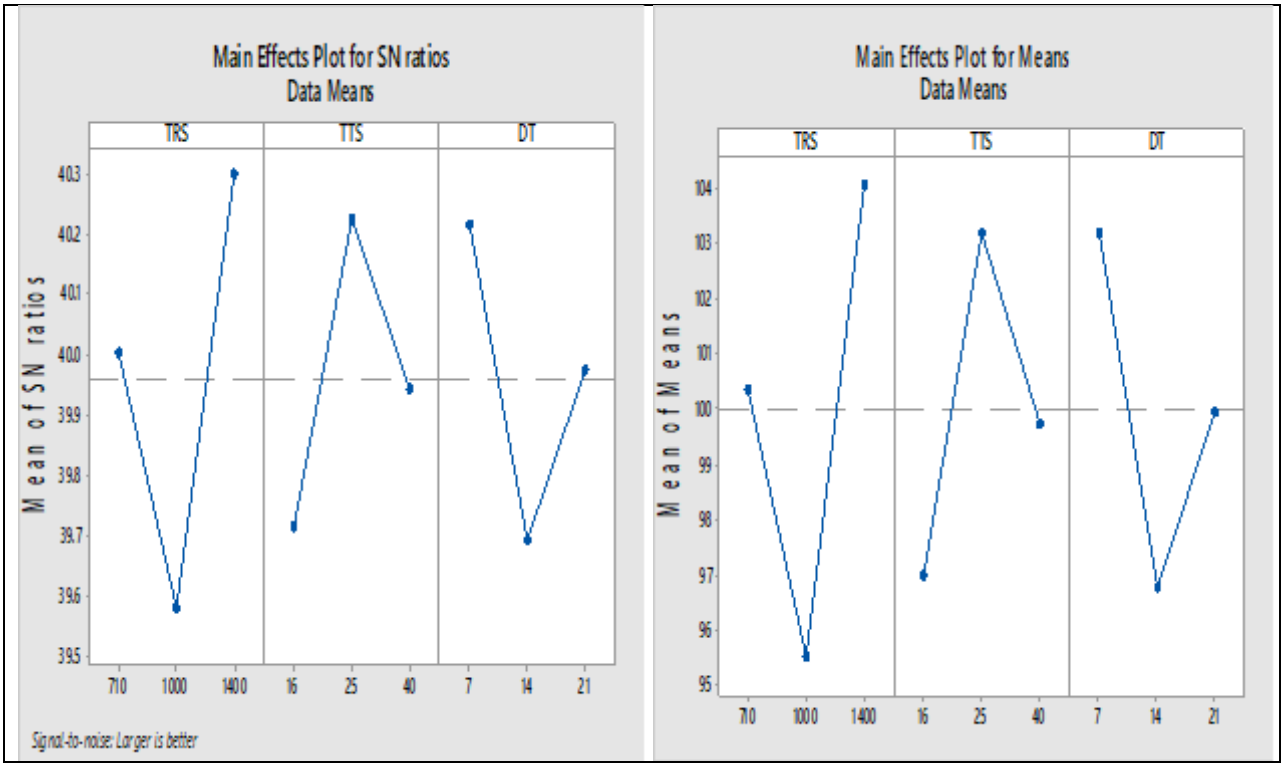

Figure 19. (a, b) Micro-hardness versus TRS, TTS, and DT

Table 5. Response table for Means Ratio (Larger is better) and Means

Response Table for Signal to Noise Ratios Larger is better			
Level	TRS	TTS	DT
1	40.00	39.71	40.22
2	39.58	40.22	39.69
3	40.30	39.94	39.97
Delta	0.72	0.51	0.52
Rank	1	3	2

Response Table for Means			
Level	TRS	TTS	DT
1	100.36	97.01	103.21
2	95.54	103.20	96.80
3	104.07	99.76	99.96
Delta	8.53	6.19	6.42
Rank	1	3	2

IV. CONCLUSION

In this research work, Taguchi's L9 orthogonal array (OA) has been used for multiple response optimization with DOE. Friction stir welding process parameters has been optimized by Taguchi's–design of experiment approach by S/N ration. Here we discuss the following conclusion that has been outcomes from the study:

- This study revealed that the utmost favourable outcomes values of the process parameters for maximum UTS and maximum value of micro-hardness were predict at TRS-1400rpm, TTS-25mm/min, DT-7s, at the 0°.
- The input parameter that has been leading for this study. The rank influences of these parameters –TTS and DT were affecting the DOE values 1.22 and 0.93, respectively as confirmation by S/N ratio.
- The input parameters predict in case 8,TRS- 1400(SN 47.60), TTS-25(SN 47.45) and DT-7(SN 47.35) shows the best optimum results.

- The temperature corresponding $T_1$and T_8 has been recorded minimum values where as T_4 and T_5 are the maximum value of temperature recorded. The reason being, the temperature variation has been more on RS and less on Advancing side because of the moment of material from AS to RS side due to tool pin rotation.
- Taguchi with the design of experts gives the best optimization solution for FSW. The experimental value has been the presence of the validation data in the expected limit range of features that determine it.
- This study advises that the difficult optimization of multi-response problems can be solved easily by Taguchi-based DOE and improve welded joint strength by optimizing the setting.

REFERENCES

1. Missori, S. and A. Sili, *Mechanical and microstructural properties of 8090 AL-LI alloy welded joints.* Metallurgical Science and Tecnology, 2002. **20**(2).
2. Alam, M.P. and A. Sinha, *Fabrication of third generation Al–Li alloy by friction stir welding: a review.* Sādhanā, 2019. **44**(6): p. 153.
3. Yan, K., et al., *Effects of Rotation Speed on Microstructure and Mechanical Properties of 2060 Al-Cu-Li Alloy in Friction Stir Welding.* Journal of Materials Engineering and Performance, 2018. **27**(11): p. 5803-5814.
4. Vigraman, T., M.V. Krishna, and M.P. Kumar, *Fine grain formation during phase transformation of a thermo-mechanically treated AA8090.* Materials Today: Proceedings, 2020.
5. Zhang, P. and M. Chen, *Progress in characterization methods for thermoplastic deforming constitutive models of Al–Li alloys: a review.* Journal of Materials Science, 2020: p. 1-20.
6. Tao, Y., et al., *Friction stir welding of 2060–T8 AlLi alloy. Part I: Microstructure evolution mechanism and mechanical properties.* Materials Characterization, 2020. **168**: p. 110524.
7. Liu, H., et al., *An effect of the rotation speed on microstructure and mechanical properties of the friction stir welded 2060-T8 Al-Li alloy.* Materials Characterization, 2017. **123**: p. 9-19.
8. Dixit, V., et al., *Influence of process parameters on microstructural evolution and mechanical properties in friction stirred Al-2024 (T3) alloy.* 2009. **14**(4): p. 346-355.
9. Arbegast, W., et al., *Hot deformation of aluminum alloys III.* 2003: p. 313.
10. Verma, S., M. Gupta, and J.P.J.P.o.t.I.o.M.E. Misra, Part G: Journal of Aerospace Engineering, *Study of thermal cycle, mechanical, and metallurgical properties of friction stir welded aviation grade aluminum alloy.* 2019. **233**(11): p. 4202-4213.
11. Verma, S. and J.J.M.T.P. Misra, *Study on temperature distribution during Friction Stir Welding of 6082 aluminum alloy.* 2017. **4**(2): p. 1350-1356.
12. Hofmann, D.C., K.S.J.M.S. Vecchio, and E. A, *Submerged friction stir processing (SFSP): An improved method for creating ultra-fine-grained bulk materials.* 2005. **402**(1-2): p. 234-241.
13. Xunhong, W., W.J.M.S. Kuaishe, and E. A, *Microstructure and properties of friction stir butt-welded AZ31 magnesium alloy.* 2006. **431**(1-2): p. 114-117.
14. Rajakumar, S., et al., *Predicting tensile strength, hardness and corrosion rate of friction stir welded AA6061-T6 aluminium alloy joints.* 2011. **32**(5): p. 2878-2890.